Increased Positive Electrostatic Potential in *p*-Hydroxybenzoate Hydroxylase Accelerates Hydroxylation but Slows Turnover[†]

Mariliz Ortiz-Maldonado, Lindsay J. Cole, Sara M. Dumas, Barrie Entsch, and David P. Ballou*

Department of Biological Chemistry, University of Michigan, Ann Arbor, Michigan 48109-0606

Received August 21, 2003; Revised Manuscript Received November 14, 2003

ABSTRACT: Para-hydroxybenzoate hydroxylase is a flavoprotein monooxygenase that catalyzes a reaction in two parts: reduction of the enzyme cofactor, FAD, by NADPH in response to binding *p*-hydroxybenzoate to the enzyme, and oxidation of reduced FAD with oxygen to form a hydroperoxide, which then oxygenates *p*-hydroxybenzoate. These different reactions are coordinated through conformational rearrangements of the isoalloxazine ring within the protein structure. In this paper, we examine the effect of increased positive electrostatic potential in the active site upon the catalytic process with the enzyme mutation, Glu49Gln. This mutation removes a negative charge from a conserved buried charge pair. The properties of the Glu49Gln mutant enzyme are consistent with increased positive potential in the active site, but the mutant enzyme is difficult to study because it is unstable. There are two important changes in the catalytic function of the mutant enzyme as compared to the wild-type. First, the rate of hydroxylation of *p*-hydroxybenzoate by the transiently formed flavin hydroperoxide is an order of magnitude faster than in the wild-type. This result is consistent with one function proposed for the positive potential in the active site—to stabilize the negative C-4a-flavin alkoxide leaving group upon heterolytic fission of the peroxide bond. However, the mutant enzyme is a poorer catalyst than the wild-type enzyme because (unlike wild-type) the binding of *p*-hydroxybenzoate is a rate-limiting process. Our analysis shows that the mutant enzyme is slow to interconvert between conformations required to bind and release substrate. We conclude that the new open structure found in crystals of the Arg220Gln mutant enzyme [Wang, J., Ortiz-Maldonado, M., Entsch, B., Massey, V., Ballou, D., and Gatti, D. L. (2002) *Proc. Natl. Acad. Sci. U.S.A. 99*, 608−613] is integral to the process of binding and release of substrate from oxidized enzyme during catalysis.

Para-hydroxybenzoate hydroxylase (PHBH)[1] from *Pseudomonas aeruginosa* and *Pseudomonas fluorescens* (EC 1.14.13.2) has been used extensively as a model for the reactions catalyzed by flavoprotein monooxygenases, particularly for enzymes that insert an atom of oxygen into the ring of a substrate (*1*, *2*). The catalytic scheme for the reaction catalyzed by PHBH shown in Figure 1 is typical of this group of enzymes. The reaction is an important transformation in one of the major metabolic pathways for the degradation of aromatic compounds by microorganisms. PHBH and probably many other enzymes of this type utilize a novel mechanism to link two rather different catalytic processes, the reduction of the flavin by NAD(P)H, followed by its reaction with oxygen to bring about hydroxylation of the substrate. The isoalloxazine ring of FAD is mobile in the enzyme and moves some 7−8 Å from an in position to an out position (ref *3* and references included). Before NADPH can reduce the flavin, the isoalloxazine of the FAD must move to the out position (see Figure 2), and this movement requires *p*-hydroxybenzoate (pOHB) to be bound to the enzyme. Then, after it is reduced, the isoalloxazine moves back to the in conformation, where the reduced flavin reacts with oxygen to initiate the second half of the catalysis—oxygenation of the substrate. This effectively gives PHBH two active sites to carry out two diverse reactions.

Our understanding of the complexity of the function of this protein has been enhanced by a structure of the mutant enzyme, Arg220Gln-PHBH, with NADPH bound (*4*). PHBH exhibits a motif for binding NADPH that has not been previously recognized in other proteins. The structure shows that reduction can only happen with the isoalloxazine out and with a rotation of the nicotinamide ring portion of bound NADPH (from a position distant from the isoalloxazine) to form a hooked conformation with the nicotinamide ring within 4 Å of the isoalloxazine. Arg220Gln-PHBH formed high quality crystals without ligands. As a result, the first structure of PHBH without a bound ligand (*4*) was solved. This structure reveals an open conformation of the enzyme that has not been observed before. This open conformation has a clear solvent path into the interior of the protein where the oxygen reactions occur and thereby provides a structural rationale for a pathway of binding and release of substrate and product from the enclosed active site. Thus, there are two potentially important protein movements to consider in the catalytic function of PHBH. First, the isoalloxazine ring

[†] Financial support was received from the U.S. Public Health Service (Grant GM 64711 to D.P.B.) and the Australian Research Council (A 09906323 to B.E.).

* To whom correspondence should be addressed. E-mail: dballou@umich.edu. Fax: (734) 763-4581. Phone: (734) 764-9582.

[1] Abbreviations: [1]PHBH, *p*-hydroxybenzoate hydroxylase; WT-PHBH, normal *p*-hydroxybenzoate hydroxylase; Glu49Gln-PHBH, mutant form of *p*-hydroxybenzoate hydroxylase; pOHB, 4-hydroxybenzoate; 2,4-DOHB, 2,4-dihydroxybenzoate; MOPS, 3-(*N*-morpholino)propanesulfonic acid.

10.1021/bi030193d CCC: $27.50
Published on Web 01/22/2004

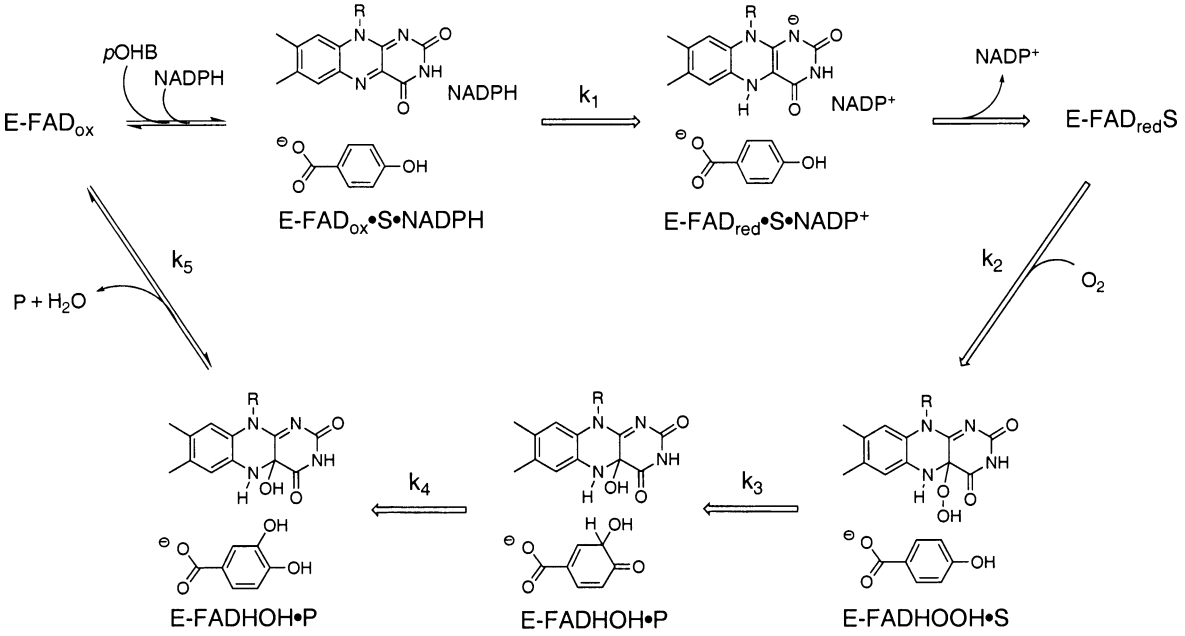

FIGURE 1: Catalytic cycle of PHBH. In the figure, E represents the enzyme, S represents pOHB, and P represents 3,4-dihydroxybenzoate, the oxygenated product. Note that k_1 to k_5 represent the rate constants for the chemical reactions in the catalytic cycle (values in Table 1).

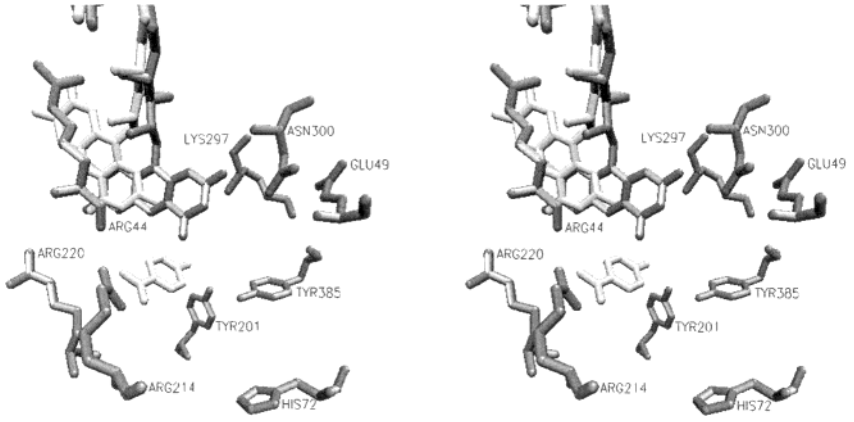

FIGURE 2: Stereoview of the active site of wild-type PHBH as the complex with pOHB (the in conformation) (*17*). The isoalloxazine ring lies over pOHB (light shading/central) in the structure illustrated. To initiate reduction, the isoalloxazine swings to the out position (exposed to solvent at the surface) that is shown by the lightly shaded isoalloxazine ring behind Arg44. The residues Tyr201, Tyr385, and His72 are involved in the H-bonding network that connects the surface to the buried phenol of the substrate.

is mobile, and this mobility is known to be fundamental to the two halves of catalysis, reduction and oxygenation (ref *3* and references therein). Then, there is the movement between open and closed conformations that may be important for substrate and product exchange and even for NADPH binding (*4*).

Electrostatic interactions are important determinants of protein function and structural integrity as described by Nakamura (*5*). However, functional roles for specific charge distributions within proteins are difficult to establish, apart from the obvious function of charge pairing in ligand binding and protein−protein interactions. In previous research, we have shown that the electrostatic field in the active site of PHBH is an important determinant of both conformational flexibility and rates of various chemical steps in catalysis (*6*). This concept was tested by mutating one of a group of positively charged residues surrounding the active site (Lys297, a buried charge, to Met297), thus decreasing the positive field around the isoalloxazine ring. The mutant enzyme, Lys297Met-PHBH, hydroxylated pOHB with a rate constant 26-fold smaller than that of WT. It was concluded that the group of positively charged residues around the isoalloxazine probably enhanced the formation of the phenolate of the substrate by lowering its pK_a. In addition, it was also proposed that the positive charge accelerated the rate of hydroxylation by stabilizing the negative charge on the flavin leaving group ($FADHO^-$) that is formed when the flavin hydroperoxide transfers oxygen to the substrate (Figure 1, k_3), thus helping to accelerate the process of hydroxylation. Lys297Met-PHBH had a diminished positive charge at the active site. The current work provides a more definitive test of the importance of this electrostatic effect on the rate of hydroxylation by PHBH by measuring the properties of an increased electrostatic field near the isoalloxazine inside the enzyme. To do this, we have constructed the mutant enzyme, Glu49Gln-PHBH, which has one less negative charge in the vicinity of the active site so that it might enhance the positive electrostatic field. The residue, Glu49, is completely conserved throughout all reported sequences of PHBH from a wide range of bacteria. It is at the end of the highly conserved loop of protein that crosses the si side of the isoalloxazine ring (residues 44−49), and it sits near the isoalloxazine ring

in the in conformation of the enzyme, where it is a buried charge and is paired with the side chain of Lys297 (see Figure 2). Circumstantial evidence thus suggests that Glu49 is as important as Lys297, which has been discussed in detail (*6*). Glu49 is also H-bonded to the amide group of Asn300, which has also been studied in relation to the function of PHBH (*7*). The mutation, Asn300Asp, like Lys297Met, decreased the positive electrostatic field next to the isoalloxazine and also caused a decrease (40-fold) in the rate of hydroxylation. The change from Glu to Gln preserves the size and shape of the residue and only changes the charge. Thus, the mutation should not have a significant impact on the structure of PHBH, although it could decrease protein stability because of charge imbalance.

This paper reports the properties of Glu49Gln-PHBH. We show that the mutant enzyme does indeed hydroxylate pOHB at a higher rate than WT-PHBH. Although in theory, this mutant could be a better enzyme than WT-PHBH, it has lost the ability in the oxidized state to rapidly exchange the product (3,4-dihydroxybenzoate) for the substrate, pOHB; therefore, in overall catalysis, it is slower. We conclude that the mutant does not rapidly equilibrate between the open and the closed conformations. A preliminary report on Glu49Gln-PHBH was presented at the 14th International Symposium on Flavoproteins in Cambridge (*8*).

MATERIALS AND METHODS

All common reagents used in this work were analytical reagent grade. NADPH used was at least 98% pure (from either Roche Biochemicals or Sigma). Other substrates for PHBH were from commercial sources and were recrystallized before use.

The construction of plasmids and the methods for expression of PHBH in *Escherichia coli* have been described previously (*7*, *9*, *10*). The WT and Glu49Gln forms of PHBH were isolated and purified as described in refs *7* and *11*.

All experimental measurements with PHBH were carried out at 3.5−4 °C to slow reactions to facilitate quantitative analysis. Some methods used were similar to those described by Moran et al. (*6*). However, the measurement of ligand dissociation constants, pK_a values of pOHB bound to enzyme, and extinction coefficient and redox potentials of the enzyme were carried out as described by Entsch et al. (*9*). Of particular importance were the buffers used for setting pH values with Glu49Gln-PHBH. For the pH range of 6.2−7.8, MOPS adjusted with NaOH was used; for the range of 7.8−8.7, Tris-sulfate was used; and for the range 9.0−9.7, glycine adjusted with NaOH was used. This mutant was inhibited by phosphate, the standard buffer used for studying most forms of PHBH, so phosphate was avoided as a buffer in experiments. Some reactions of reduced enzyme with oxygen were carried out in phosphate buffer because it was found that phosphate inhibited the reduction with NADPH and not the second part of catalysis (see Results). All kinetic data were collected with a Hi-Tech Scientific Model SF-61 stopped-flow spectrophotometer in either absorbance or fluorescence modes. Rapid reaction kinetic traces were analyzed and simulated with the software Program A, an MS-DOS based series of programs developed in our laboratory by Rong Chang, Chung-Yen Chiu, Joel Dinverno, and David Ballou, University of Michigan. Analysis is based upon the Marquardt algorithm for fitting data to sums of exponentials (*12*).

Electrostatic potential distributions within PHBH were calculated using the program Adaptive Poisson−Boltzmann Solver (*13*). Charges for amino acids were taken from charge files compiled for the modeling package, AMBER (*14*). The adenosine, pyrophosphate, and ribityl portions of FAD were taken from chemically similar examples in charge files for *t*RNA that have been compiled for AMBER. Charges for the isoalloxazine of FAD and pOHB were taken from previous ab initio calculations (*6*). The electrostatic calculations for WT were performed using the protein dimer as defined in the paper by Weijer et al. (*15*). The calculations for Glu49Gln-PHBH used the same structure as WT-PHBH without energy minimizations. The potential was calculated for all points in a grid with spacing of 2.23 Å within a cube of 145 Å per side using boundary conditions of zero charge. The protein dimer was centered within the box. The radius of each atom within the cube was defined as its van der Waals radius. Solvent was modeled as a continuum with a dielectric constant of 80. Solvent accessibility to the protein was calculated using a radius of 1.4 Å. Solvent was assumed to contain monovalent ionic charges and an ionic strength of 0.145 M. Accessibility of ionic species was calculated using a radius of 2.0 Å.

RESULTS

Purification and Properties of Glu49Gln-PHBH as Compared to WT-PHBH. The mutant enzyme was less stable than WT enzyme at any given temperature and was difficult to use. To obtain useful yields of functional Glu49Gln-PHBH by expression in *E. coli*, growths were carried out at 25 °C. With the growth of cells at 37 °C, most of the mutant protein expressed was present as insoluble inclusion bodies. Extraction of WT-PHBH from *E. coli* can be carried out at room temperature, but the mutant enzyme had to be prepared at about 5 °C to obtain adequate yields. In contrast to the WT enzyme, when isolated, Glu49Gln-PHBH had pOHB bound to some fraction of the enzyme, consistent with the later discovery that this mutant exchanges pOHB slowly. In the solution conditions commonly used to handle WT-PHBH (such as 25 °C and pH 6.5), the mutant slowly (over minutes to hours) forms a precipitate. At 4 °C, the denaturation process is much slower, and the protein was used successfully in experiments at this temperature. The mutant enzyme remained in solution for longer periods at higher pH values. It was discovered that including 5% glycerol helped to prevent precipitation of Glu49Gln-PHBH, thus making experimental analysis effective, particularly at pH 6.5. These properties are in contrast to the less positively charged Lys297Met-PHBH, which was at least as stable as the WT enzyme (*6*). Lys297 is the positive partner to Glu49 in a buried charge pair (see Figure 2).

A summary of some key properties of the mutant as compared to WT enzyme is shown in Table 1. Below pH 8, the mutant enzyme is as effective as the WT enzyme in conversion of pOHB to product—for each NADPH oxidized, a molecule of 3,4-dihydroxybenzoate is produced. Above pH 8, Glu49Gln-PHBH forms more 3,4-dihydroxybenzoate per molecule of NADPH than WT-PHBH (as shown in Table 1, pH 8.6). However, as a catalyst, it functions at only 3−4%

Table 1: List of Key Experimental Parameters Used in Comparing the Properties of WT and Glu49Gln Forms of PHBH

property	WT-PHBH	Glu49Gln-PHBH
extinction coefficient, 450 nm (peak), pH 6.5 ($mM^{-1}\,cm^{-1}$)	10.3	10.4
K_d, pOHB (4 °C, pH 6.5) (μM)	9.5 ± 0.5	<5
K_d, 2,4-DOHB (4 °C, pH 6.5) (μM)	22 ± 1.5	32 ± 2
K_d, NADPH (4 °C, pH 6.5) (μM)	210 ± 10	74 ± 4
pK_a for Eox•pOHB complex	7.5 ± 0.1	>9.5
Em,7 enzyme (mV)	−163 ± 1.5	−156 ± 1.5
Em,7 enzyme + pOHB (mV)	−165 ± 1.5	−164 ± 1.5
% hydroxylation, pH 6.5, 25 °C[a]	100 ± 1[b]	100 ± 1
pH 7.9, 25 °C	98 ± 1[b]	98 ± 1
pH 8.7, 25 °C	86 ± 1[b]	94 ± 1
K_d, Br^- (active site binding) (mM)	4.6 ± 0.2[b]	0.50 ± 0.025
K_d, E• pOHB + Br^- (active site binding) (mM)	2.3 ± 0.1[b]	0.14 ± 0.01
turnover (saturating pOHB, NADPH, 0.25 mM oxygen)		
pH 6.5°, 4 °C (s^{-1})	6.2 ± 0.2	0.2 ± 0.02[c]
pH 8.6, 4 °C (s^{-1})	7.5 ± 0.2[b,d]	1.5 ± 0.15[c]
rate constants shown in Figure 1 measured at pH 6.5, 4 °C		
k_1 (s^{-1})	50 ± 1.5	1.5 ± 0.04
k_2 ($M^{-1}\,s^{-1}$)	2.8 × 10^5	1.8 × 10^5
k_3 (s^{-1})	45 ± 1.5	≥ 180
k_4	≫k_3	≫k_3
k_5 (s^{-1})	14 ± 0.3	11 ± 0.3

[a] The values for percent hydroxylation were obtained by measuring either the amount of NADPH consumed in turnover of a known, limiting amount of pOHB or the amount of 3,4-dihydroxybenzoate formed in an oxygen half-reaction. [b] These values for WT were determined as part of this paper. The other values for WT come from previously published work, reported in ref *9*. [c] These values were obtained by steady-state analysis of substrate dependence. [d] This value was obtained from an experiment to measure turnover by using the technique of enzyme-monitored turnover (*35*).

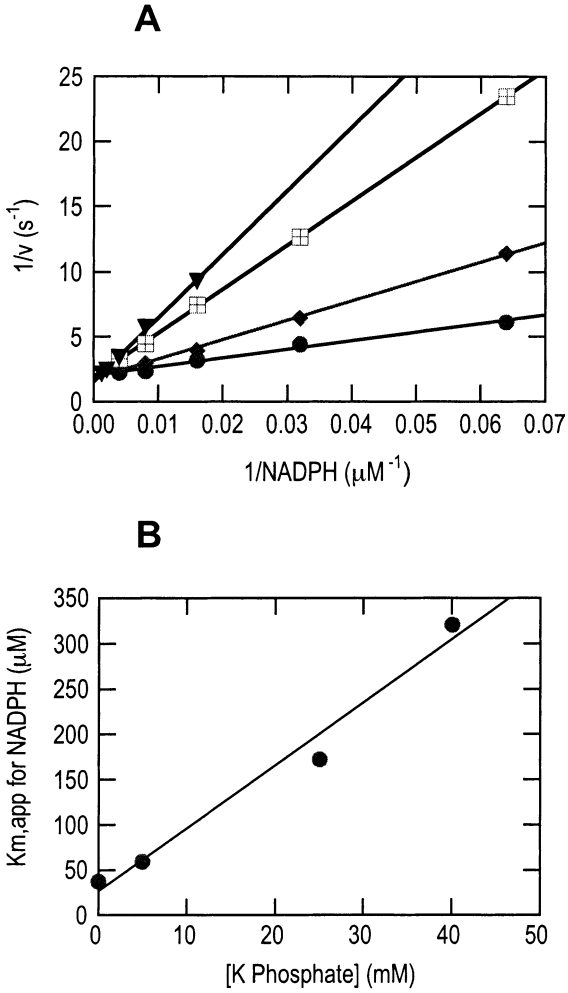

FIGURE 3: Phosphate inhibition of Glu49Gln-PHBH. Inhibition was analyzed by steady-state kinetics. Reaction solutions contained 1.0 μM enzyme, 500 μM pOHB, and varying [NADPH] in 50 mM MOPS buffer equilibrated with air, pH 6.8 at 4 °C. (A) Lineweaver−Burk plots are shown for the dependence of enzyme activity on NADPH concentration over a number of different concentrations of phosphate (shown in panel B). The raw rate data were collected with a stopped-flow spectrophotometer and analyzed by nonlinear regression (using KaleidaGraph), then transformed into double-reciprocal plots for illustration. (B) Shows the linear relationship (simple competitive inhibition) between apparent K_m values for NADPH (from the slopes of the primary plots) and phosphate concentration. A K_i value for the phosphate of 4.3 mM was obtained from the slope and intercept.

of WT rate at pH 6.5 but improves to 20% at pH 8.6. The redox potential of free mutant enzyme (−156 mV) is slightly more positive than WT enzyme (−163 mV), consistent with a more positively charged environment around the isoalloxazine ring. This difference in redox potential disappeared with pOHB bound—both mutant and WT enzymes were the same within experimental error (−165 mV). An important difference between mutant and WT enzymes (consistent with a more positively charged active site) is their behavior with anions. For example, Glu49Gln-PHBH forms stronger complexes with bromide (Table 1) than does WT-PHBH. Unlike WT, the mutant enzyme is also inhibited by phosphate, which has been the buffer of choice in most studies of PHBH. Phosphate was found to be an inhibitor competitive for NADPH with an apparent K_i of 4.3 mM (Figure 3), similar to the K_i for chloride inhibition of WT (*16*). Anions such as chloride and bromide bind in the positively charged active site of WT-PHBH and modify the spectrum of the flavin (*17*, *21*). No clear, active site binding of phosphate can be measured with WT-PHBH. Thus, phosphate could only be used as a buffer ion with Glu-49Gln-PHBH with caution, as is the case with small anions such as chloride with WT-PHBH (*16*). Because of the inhibition by phosphate, this buffer was replaced by solutions of MOPS to study the mutant enzyme. Interactions between Glu49Gln-PHBH and substrates are very similar to those of WT (see Table 1). When pOHB is bound to the mutant enzyme, the difference spectrum is the same as for WT, consistent with the flavin positioned in the in conformation (*17*). An exact K_d is not reported in Table 1 (<5 μM) because the value is too small for accurate determination using absorbance spectrophotometry, and it cannot be determined using fluorescence techniques because the buffer (MOPS) quenches any signal. When 2,4-DOHB is bound to the mutant enzyme, the difference spectrum is again the same as that for WT-PHBH, consistent with the flavin being positioned in the out conformation (*17*). These observations suggest that the mutation did not cause significant structural changes to the arrangement of residues in the active site. One property is apparently inconsistent with a more positively charged active site—the pK_a of the phenol of pOHB bound in the active site of the oxidized enzyme has risen from 7.5 (the value in WT-PHBH) to a value greater than 9.5 in Glu49Gln-PHBH (Table 1). The enzyme rapidly denatures above pH 9.5, and this property prevented the observation of static difference

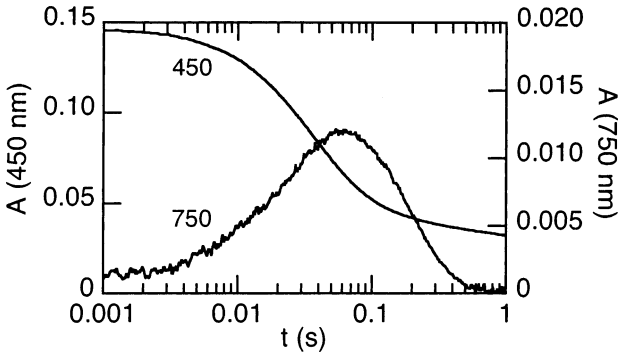

FIGURE 4: Absorbance changes in Glu49Gln-PHBH upon reduction with NADPH at pH 9.5. A solution of 14 μM enzyme and 0.5 mM pOHB in an anaerobic solution of 50 mM glycine adjusted to pH 9.5 (with NaOH) at 4 °C was mixed with an anaerobic solution of 2.0 mM NADPH in the same buffer. Flavin reduction is shown by the large decrease in absorbance at 450 nm, which corresponds to the small absorbance increase at 750 nm, due to the formation of the charge-transfer band between NADP and $FADH^-$ (*19*).

spectra at high pH to determine a p*K*a for dissociation of pOHB (*9*).

Analysis of the Reductive Half-Reaction. The reduction of Glu49Gln-PHBH was studied by mixing the enzyme in a complex with pOHB with solutions of NADPH under anaerobic conditions in the stopped-flow spectrophotometer. The observed rates of reduction were measured by following the absorbance at 450 nm for a range of concentrations of NADPH. From this information, the rate constant for reduction of enzyme saturated with NADPH (k_1 in Figure 1), and the dissociation constant for NADPH was calculated as described before (*18*, *19*). At pH 6.5 and 4 °C, the rate constant for reduction of enzyme-bound FAD by NADPH was much slower than for WT-PHBH (1.5 s^{-1} as compared to 50 s^{-1}), and the measured K_d for NADPH was 3-fold smaller than for WT-PHBH (see Table 1). It has been shown that charge-transfer absorption bands are an indication of the optimum alignment of NADPH to FAD for reduction in this enzyme (*19*). At pH 6.5, when the reduction was followed at wavelengths longer than 550 nm, there was no observed change in absorbance with Glu49Gln-PHBH. This is consistent with no detectable formation of charge-transfer interactions during reduction, in contrast to WT-PHBH at pH 6.5 (*20*), which reduces at a high rate and expresses absorbance changes beyond 550 nm. However, when the rate of reduction of the mutant enzyme was measured at pH 9.5 in glycine buffer, the rate constant was 32 s^{-1}, only 2.5-fold slower than WT-PHBH under the same conditions (see Figure 4, 450 nm trace). Rates of reduction between pH 6.5 and 9.5 were intermediate between 1.5 and 32 s^{-1}. Because the increase in the rate of reduction had not approached a limiting value at pH 9.5, the highest pH that was practical to use to study the enzyme, the nature of the pH-dependent process in reduction of Glu49Gln-PHBH was not clear. However, the variation in rate constant with pH was consistent with a process involving a single deprotonation, and the actual maximum rate constant for reduction could be the same (or greater) than the maximum rate for WT-PHBH. When the reduction of Glu49Gln-PHBH at pH 9.5 was measured at wavelengths longer than 550 nm, absorbance was observed to increase and decrease in the time frame of reduction (Figure 4—750 nm). This observation was consistent with the formation of charge-transfer interactions on the pathway to reduction of the flavin. At 750 nm, the charge-transfer interaction is dominated by the complex between NADP and $FADH^-$ (*19*). At pH 6.5, the reduction of flavin is the rate-determining step in the reductive half of catalysis, as measured in stopped-flow experiments (see Figure 1). At pH 9.5, the rate-determining step has changed from reduction of FAD to the release of NADP from the enzyme (7.0 s^{-1}, as measured by the rate of decay of absorbance at 750 nm—see Figure 4). This is similar to the behavior of WT-PHBH at pH 8.0 (*18*). However, with WT-PHBH under these conditions, the rate of release of NADP from the enzyme is largely rate-determining in overall catalysis (as shown also by the turnover value of 7.5 s^{-1} at pH 8.6 for WT-PHBH in Table 1).

Analysis of the Oxygen Half-Reaction. The second half of catalysis occurs when the reduced enzyme in complex with pOHB reacts with oxygen after NADP has dissociated from the enzyme (see Figure 1). This process was followed in the stopped-flow spectrophotometer by mixing an anaerobic solution of reduced enzyme in complex with pOHB with solutions of buffer containing various concentrations of oxygen. The changes were measured using absorbance and fluorescence spectroscopy. By measuring absorbance, the characteristic transient flavin derivatives with oxygen formed during the reaction (the C4a-hydroperoxide and the C4a-hydroxide as shown in Figure 1) can be identified (*21*). By fluorescence, the rate of formation and decomposition of flavin-C4a-hydroxide can be followed because this species has been shown to be substantially more fluorescent than any other chemical species in the oxygen reactions of PHBH (*6*).

At pH 6.5 and 4 °C, absorbance changes observed in the reaction over a range of wavelengths from 340 to 520 nm appeared to be very similar to those of WT-PHBH. There was a fast initial, oxygen-dependent reaction to form the flavin-C4a-hydroperoxide (see Figures 1 and 5A,B) with a second-order rate constant similar to that of WT-PHBH (see Table 1). After the oxygen-dependent reaction, a large increase in absorbance was observed between 425 and 490 nm (and a decrease in absorbance between 385 and 410 nm) that is due to the formation of oxidized flavin at a rate of 11 s^{-1}, similar to that of WT (see Figure 5B). In the WT reaction, an intermediate phase (occurring between the second-order reaction with oxygen to form the hydroperoxyflavin and the return to oxidized flavin), represented by a small change in the absorbance traces, was proven to correlate with hydroxylation [transfer of oxygen to pOHB (*21*, *22*)—k_3 in Figure 1]. This small change in absorbance was shown to be due to conversion of the flavin-C4a-hydroperoxide to the flavin-C4a-hydroxide. This formation of the flavin-C4a-hydroxide as oxygen is transferred to pOHB is also accompanied by a large increase in fluorescence (*6*) followed by a corresponding large decrease in fluorescence as oxidized flavin is formed. The fluorescence changes provide a unique, convenient, and sensitive marker of hydroxylation. We were unable to observe an intermediate (hydroxylation) phase in absorbance traces in the reactions of Glu49Gln-PHBH. Instead, there was a small phase with a rate of $\sim$6 s^{-1} that followed the formation of oxidized flavin (as can be seen in the 420 nm trace in Figure 5B). When the same reactions with Glu49Gln-PHBH were followed by fluorescence, it was clear that hydroxylation had occurred

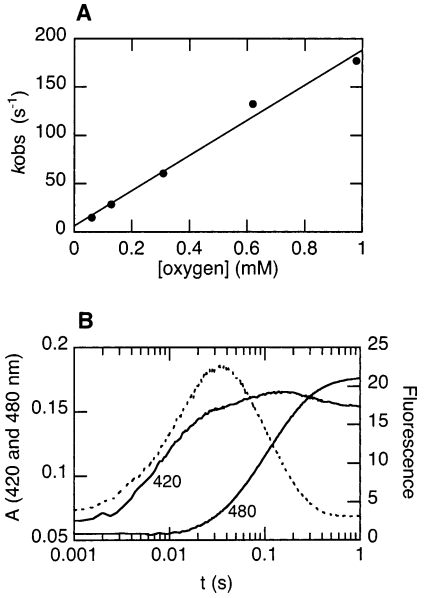

FIGURE 5: Absorbance and fluorescence changes upon reacting reduced Glu49Gln-PHBH in complex with pOHB with oxygen at pH 6.5 and 4 °C. The final reaction contained 22 μM mutant enzyme (absorbance) or 9.6 μM (fluorescence), 0.5 mM pOHB, oxygen, 50 mM phosphate as the K salt, 0.5 mM EDTA, pH 6.5. (A) The relationship between oxygen concentration and rate of formation (1.8×10^5 M^{-1} s^{-1}) of the flavin hydroperoxide (Figure 1, k_2) as determined from the reactions observed at 415 nm (not shown in Figure). (B) All reactions contained 0.63 mM oxygen. Absorbance traces at 420 (absorbance expanded by a factor of 2 for comparison) and 480 nm (full lines) that illustrate four detectable phases in the reaction to form oxidized enzyme. The fluorescence trace (dotted line) was the emission signal at >510 nm caused by excitation at 400 nm. Two phases were detected, and these correspond to two phases in absorbance.

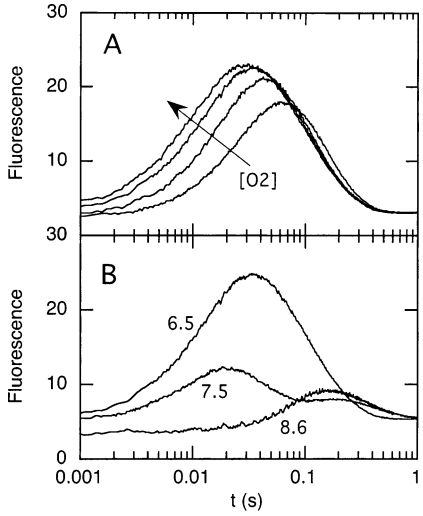

FIGURE 6: Use of fluorescence spectroscopy to analyze the reaction when reduced Glu49Gln-PHBH in complex with pOHB is mixed with a solution containing oxygen. (A) A solution of 9.6 μM reduced enzyme in complex with 0.5 mM pOHB in 50 mM phosphate as the K salt, 0.5 mM EDTA, pH 6.5 and 4 °C was mixed with solutions of the same buffer containing specific concentrations of oxygen. Fluorescence emission was detected at wavelengths >510 nm after excitation at 400 nm. Reaction traces shown contained 0.125, 0.32, 0.63, and 0.98 mM oxygen in the reaction. Two reactions dominate—a fast almost second-order hydroxylation process followed by the oxygen independent decomposition of the flavin C4a-hydroxide (see Figure 1). (B) Reaction traces recorded at constant oxygen concentration (0.63 mM) but varying pH. To change pH, separate experiments were carried out with different buffer solutions as described in Materials and Methods. The pH used to collect each trace is shown by the numbers beside the trace. The fast increase in fluorescence easily observed at pH 6.5 occurs at a constant rate at all pH values—this phase decreases in amplitude as the pH rises because the second reaction (decrease in fluorescence at pH 6.5) becomes faster with increasing pH. At high pH (8.6), two slower reactions (with small amplitudes in fluorescence) that are not detected in the 1 s time frame at pH 6.5 are observed (with rate constants of 7 and 3.5 s^{-1}). These reactions correspond to oxidized enzyme in absorbance and have no dependence on oxygen concentration.

very rapidly. For example, a trace of fluorescence excitation at 400 nm and with detection of emission beyond 510 nm is shown in Figure 5B. It was a surprise to find that the large increase in fluorescence (characteristic of the hydroxylation reaction) is nearly coincident with the absorbance increase due to formation of the flavin hydroperoxide, and this fluorescence increase also showed strong dependence on oxygen concentration (see Figure 6A). Note that the large fluorescence signal decays in the same time frame as the formation of oxidized flavin as seen by the large increase at 480 nm (Figure 5B). These observations can only be possible if the hydroxylation rate in this mutant is at least as fast as the initial oxygen reaction under the conditions studied. It was not possible to increase oxygen concentration beyond approximately 1 mM after mixing because of the limited solubility of oxygen in buffer. Thus, we could not push the second-order reaction with oxygen to higher measured rates to separate out the following hydroxylation reaction. Even if this technical barrier could be overcome, the rate of hydroxylation would be too great to be measured in a stopped-flow spectrophotometer. We estimated that hydroxylation by the mutant was occurring with a rate constant ≥ 180 s^{-1} and is limited by the rate of formation of the flavin-C4a-hydroperoxide. Because the WT has a rate of hydroxylation of 45 s^{-1} at pH 6.5, we concluded that the mutant enzyme hydroxylates pOHB at a greater rate than does WT-PHBH. Additional support for this conclusion came from analysis of the same oxygen half-reaction in the presence of 0.1 M sodium azide. It has been shown that the rates of the oxygen reactions of PHBH are modulated by anions that bind in the active site (*21*). The initial reaction of oxygen with reduced enzyme is not changed by the presence of anions such as azide, but the rates of hydroxylation and the subsequent loss of water to form oxidized flavin are substantially slower. In the case of WT-PHBH, 0.1 M azide slows the hydroxylation rate to 7 s^{-1} (*21*). Fluorescence was used to follow hydroxylation by the mutant enzyme (similar to Figure 6A). As in the reaction without azide, the hydroxylation process was also dependent upon oxygen concentration. By analogy to the reactions without azide, we concluded that (even in the presence of azide) hydroxylation was occurring at a rate of ≥ 180 s^{-1}. Thus, the actual rate constant is at least 25-fold greater than that of WT-PHBH under the same conditions. The small phase in absorbance traces (after formation of oxidized flavin) in the reaction by the mutant enzyme (the small down in the trace for 420 nm between 0.2 and 1 s in Figure 5B—mentioned above) is due to the release of the product, 3,4-dihydroxy-benzoate, from the enzyme (see also later results). This conclusion is also consistent with the observation of only two measurable phases in fluorescence—formation and decomposition of the C4a-hydroxyflavin (see Figure 5B). We know that the

fluorescence signal is due to the presence of the hydroxyflavin (as explained before), and the data show that rearrangement of the aromatic product (shown by k_4 in Figure 1) has little or no influence upon fluorescence or absorbance signals. The nonaromatic product formed in reaction k_3 in Figure 1 should have absorbance in the range of 350−400 nm (*21*). Thus, the rearomatization reaction (step k_4) must be too fast for the nonaromatic intermediate to accumulate, just as was found for WT-PHBH with pOHB (*21*).

To be sure that the high rate of hydroxylation at pH 6.5 was not some fortuitous maximum in the pH dependence for hydroxylation by the mutant enzyme as compared to WT enzyme, we studied the oxygen reaction over a range of pH values from 6.0 to 8.6. The results are best illustrated by three fluorescence traces in experiments designed to follow the formation and decay of the flavin hydroxide (Figure 6B). In the time period of 1−100 ms, two phases are observed, as discussed above for pH 6.5. The faster phase at each pH (fluorescence increase) corresponded both to the rate of formation of the flavin hydroperoxide and to its transformation into the flavin hydroxide. This rate remained constant with pH, and the two processes could not be differentiated. The next phase (fluorescence decrease) is due to the decomposition of the flavin hydroxide, and this increases in rate with pH, as has been observed before with this enzyme (*23*). Thus, as pH increases, the maximum amplitude in the fluorescence signal decreases because the maximum amount of flavin hydroxide formed transiently is less. By pH 8.6, the fluorescence signal due to flavin hydroxide was no longer detectable because it decayed so rapidly (see Figure 6B). However, hydroxylation was occurring as shown by the measurement of 94% product formation at this pH (Table 1). It was not possible to measure directly the dependence of the rate of hydroxylation on pH because it occurred at the same rate as the formation of the flavin-C4a-hydroperoxide (as discussed above for pH 6.5). The small, slower phase causing an increase in fluorescence signal that can be seen at both pH 7.5 and (more prominently) pH 8.6 is discussed in the next paragraph.

Unfortunately, this picture of a mutant enzyme that hydroxylates substrate faster than the WT enzyme is countered by the fact that overall turnover is slow (see above and Table 1). At pH 6.5, it is tempting to suggest that the rate-determining step in turnover is the relatively slow reduction of flavin. However, the reduction rate constant (1.5 s^{-1}) is 7.5-fold greater than the measured turnover rate (0.2 s^{-1}), and reduction is much faster at higher pH values. When the enzyme is directly monitored during steady-state turnover at 450−480 nm (where enzyme absorbance is dominated by oxidized flavin), the enzyme is >90% oxidized in steady-state (see Figure 7). Thus, the slow processes in turnover involve oxidized enzyme. Because reduction is not rate determining, it is likely that either the process of product release after the reaction with oxygen or substrate binding to initiate catalysis is limiting turnover. In the reactions with oxygen at pH 6.5 between wavelengths of 420 and 500 nm, very small absorbance changes were observed with a rate of ~0.3 s^{-1} (see end of 480 nm trace in Figure 5B where absorbance is still increasing after 1 s). The rate of this slow phase was independent of the concentration of pOHB. In previous studies of the oxygen reactions of PHBH, a similar slow phase has been observed. However, unlike the experiments reported here, the rate of the slow phase was dependent upon pOHB concentration and was due to pOHB trapping some flavin hydroxide after release of product. The small, slow absorbance changes after the formation of oxidized Glu49Gln-PHBH were kinetically equivalent to small changes in fluorescence that could only be observed clearly at higher pH values (Figure 6B—note the trace at pH 8.6 where the flavin-C4a-hydroxide is kinetically invisible). These slow phases detected by absorbance and fluorescence increased in rate as pH increased. At pH 8.6 (Figure 6B), the slowest phase observed by fluorescence is 3.5 s^{-1}. The origins of these slower processes were studied in more detail to try to understand the limits to turnover by this mutant enzyme.

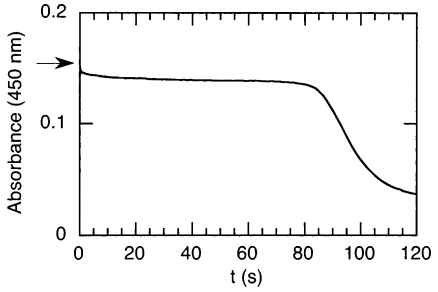

FIGURE 7: Enzyme-monitored turnover reaction for Glu49Gln-PHBH. The behavior of the enzyme was measured at 450 nm using the method described by Gibson et al. (*35*). The final reaction solution in the stopped-flow spectrophotometer contained 15 μM enzyme, 0.4 mM pOHB, 1.5 mM NADPH, and 260 μM oxygen in 50 mM MOPS, pH 6.5 at 4 °C. During steady state when there is almost no dependence on substrate concentrations (long flat part in the absorbance trace), the enzyme is at least 90% in oxidized forms.

Binding and Dissociation of Substrate and Product. Glu49Gln-PHBH was different from WT-PHBH when it bound pOHB to the oxidized enzyme—the normal process to initiate catalysis. WT enzyme binds to pOHB too fast to be measured, even at 4 °C in a stopped-flow spectrophotometer (*21*). However, some mutants of PHBH have been studied that exhibit much slower rates of binding between oxidized enzyme and pOHB (*6*, *7*). The interaction between Glu49Gln-PHBH and pOHB was studied at pH 6.5 and in MOPS buffer by following absorbance changes of FAD at 481 (Figure 8A) and 391 nm (data not shown). Unlike WT-PHBH, the full change in absorbance with binding was observed. In Figure 8A, four traces illustrate the absorbance changes over a wide range of pOHB concentrations. Two phases are observed—a fast, second-order reaction (dominating the observed absorbance change) and a much slower, first-order reaction that is independent of pOHB concentration (very small decrease in absorbance in Figure 8A). Analysis of the first phase gave a rate constant of association of 1.3×10^5 M^{-1} s^{-1}, which was slower than for WT-PHBH (>10^6). The second phase occurred with a first-order rate constant of ~0.3 s^{-1}, which corresponds with the rate of the last small change in absorbance observed after formation of oxidized enzyme in the oxygen half-reactions.

The rate of dissociation of product from oxidized enzyme was followed also at pH 6.5 by absorbance at 501 and 385 nm. At these wavelengths, there are significant differences between the spectra of enzyme with pOHB bound as compared to enzyme with 3,4-dihydroxybenzoate bound. By starting with the enzyme in complex with 3,4-dihydroxybenzoate (the state of the enzyme after the flavin has oxidized

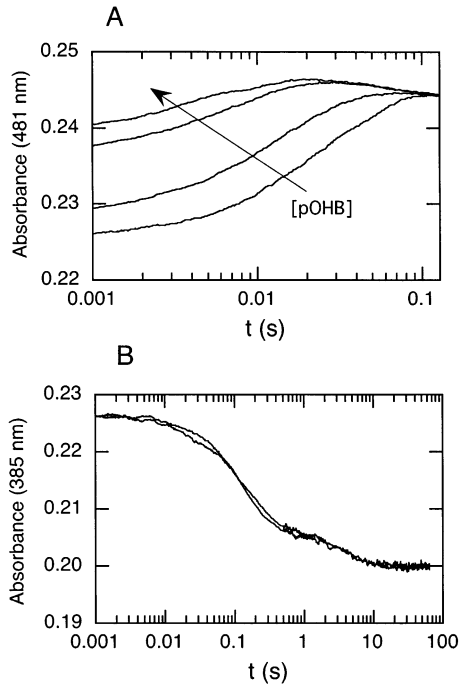

FIGURE 8: Kinetics of binding substrates to oxidized Glu49Gln-PHBH. Reactions were carried out by mixing oxidized enzyme with different concentrations of substrate. (A) The final reaction conditions were 29 μM enzyme in 50 mM MOPS, pH 6.5 and 4 °C, with one of the following concentrations of pOHB—0.25, 0.5, 1.25, and 2.5 mM. Reactions were measured at 481 nm. The observed rates of the fast phase were proportional to the concentration of pOHB, and the slope gave a second-order rate constant of 1.3×10^5 M^{-1} s^{-1}. The fast phase was followed by a small decrease in absorbance in the time frame of the slow process in panel B. (B) In these reactions, there was 29 μM enzyme complexed with 3,4-dihydroxybenzoate (0.5 mM)—the product of catalysis under the same conditions as above. Two traces are shown where the enzyme with product was mixed with either 2 or 8 mM pOHB, and the reaction was followed at 385 nm. The reaction traces were noisy because of some turbidity from a little enzyme precipitation. Both phases were independent of the concentration of pOHB—the faster phase had a measured rate constant of 6−7 s^{-1} (note the different time scale as compared to panel A), and the slower small phase had a rate constant of 0.25−0.3 s^{-1}.

in the oxidative half-reaction), and mixing with solutions of pOHB, it was possible to measure the rate of dissociation of product (see Figure 8B). This figure shows that two processes were measured in this experiment and they were both independent of pOHB concentration. The larger, faster phase with a rate of 6−7 s^{-1} must be product dissociation because this rate corresponds with the small decrease in absorbance at 420 nm in the oxygen reaction following formation of oxidized flavin (Figure 5B—0.2−1 s) at a rate of 6 s^{-1}. This process is 30-fold faster than the measured rate of turnover (Table 1). The second, slower phase (Figure 8B) has a rate of 0.25−0.3 s^{-1}, equivalent to the slow phase for binding pOHB to the enzyme and just a fraction faster than turnover (Table 1). Thus, a slow process in the binding of pOHB is responsible principally for the slow turnover rate at pH 6.5.

The catalytic turnover rate by Glu49Gln-PHBH increases with increasing pH to a value of 1.5 s^{-1} at pH 8.6 (Table 1). There are three processes in the transient kinetics of the mutant enzyme that can account for this turnover rate at pH 8.6. Release of NADP after reduction of the enzyme occurs at a rate of 7 s^{-1} (the decrease in absorbance at 750 nm in Figure 4). In the oxygen reactions, two processes are observed by fluorescence after the formation of oxidized flavin (as seen by the pH 8.6 trace in Figure 6B and discussed previously) with first-order rate constants of 7 and 3.5 s^{-1}. If these three processes are on the catalytic pathway at pH 8.6, then together they predict a V_{max} of 1.75 s^{-1}. This is slightly greater than the measured rate (1.5 s^{-1}), which was not extrapolated to infinite oxygen concentration. We concluded that the small changes in fluorescence at pH 8.6 in Figure 6B are on the catalytic pathway and probably represent the dissociation of 3,4-dihydroxybenzoate from and the binding of pOHB to the oxidized enzyme. Thus, the primary limiting factor in turnover at pH 8.6 is the same process as at pH 6.5—the slow, conformational change required for binding pOHB (Figure 8B), except that this process is an order of magnitude faster at pH 8.6 than at pH 6.5.

DISCUSSION

The objective of the research reported in this paper was to test the hypothesis (*6*) that the highly conserved positively charged residues (Arg220, Arg214, Arg44, and Lys297) that surround the active site of PHBH are important in enhancing the core hydroxylation reaction in catalysis by providing a positive electrostatic field about the isoalloxazine. The hypothesis was based upon the idea that a positive electrostatic field would stabilize the $FADHO^-$ (alkoxide) leaving group during transfer of oxygen from the C4a-hydroperoxide (Figure 1) and also promote deprotonation of pOHB to form the more nucleophilic phenolate. This hypothesis was previously tested with the mutation Lys297Met (*6*). Lys297 was the only positive residue (of the group above) that could be changed to alter the electrostatic field without disrupting other aspects of catalysis. As predicted, this change caused a decrease in the rate of hydroxylation (*6*), but it was recognized that a decrease in the rate of hydroxylation might also be attributed to factors other than the decrease in positive charge. Another test of this hypothesis would be to examine whether an increase in the positive field in the active site would increase the rate of transfer of oxygen to pOHB.

By constructing Glu49Gln-PHBH, we have created a form of PHBH that has an increased positive charge and indeed does have enhanced oxygenase activity. We could not measure the full magnitude of the enhancement because of the limitations discussed in the Results. However, the minimum increase in hydroxylation rate is 4-fold but could be as high as 26-fold. Three other notable changes were observed when this mutant enzyme was compared to WT-PHBH. First, it is less stable than WT-PHBH. Second, the pK_a of pOHB bound to the enzyme is greater than for WT-PHBH. Finally, the mutant enzyme is a poor catalyst as compared to WT enzyme because it binds the substrate slowly in a process that determines the overall rate of catalysis (Figure 8). Thus, it is not surprising that Glu49 is absolutely conserved in alignments of the sequences of PHBH from many different bacteria.

The electrostatic field of the buried active site of Glu49Gln-PHBH can be calculated using the program Adaptive Poisson−Boltzmann Solver (*13*) to provide an approximate solution to the Poisson−Boltzmann equation for the protein in a continuum that represents the solvent. The results of

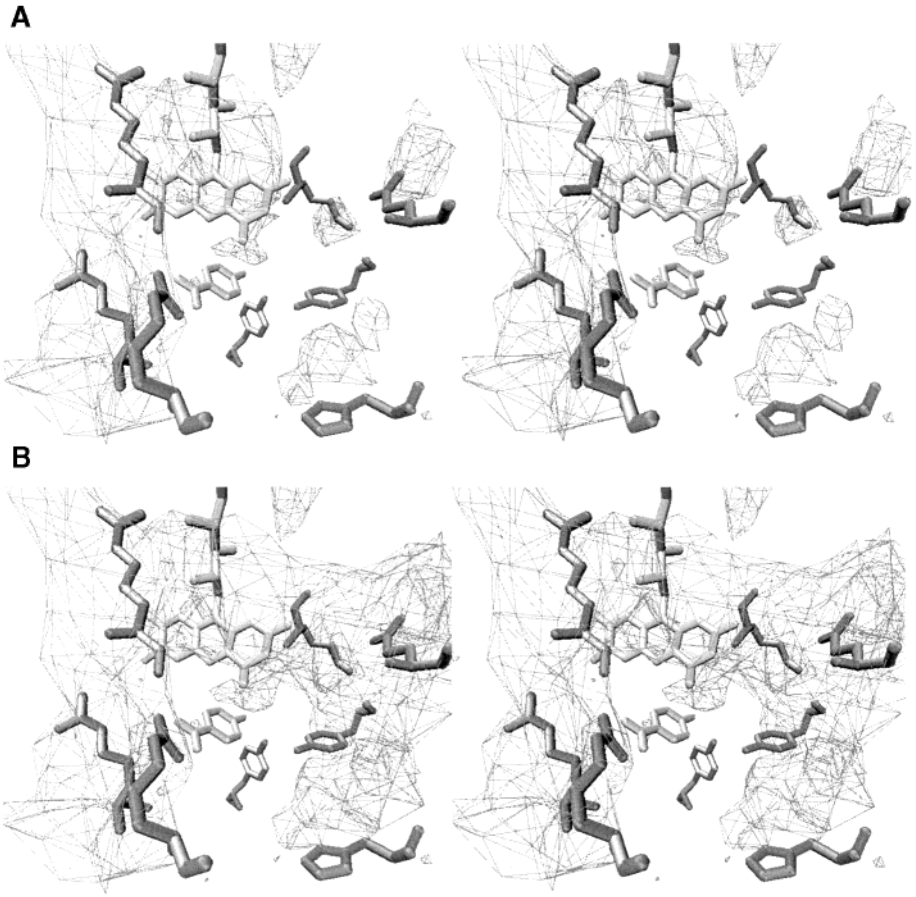

FIGURE 9: Calculated estimates of the electrostatic charge environment of the active site of PHBH. Charge distribution was computed using the program Adaptive Poisson−Boltzmann Solver as described in Materials and Methods. (A) The active site of the WT enzyme with the flavin sitting in the in conformation (same orientation as in Figure 2). The wire-framed surface encloses volumes of positive potential ≥30 kT/e. (B) The same view as panel A of the active site of the Glu49Gln enzyme (based on the assumption of no significant rearrangements), where the wire-framed surface encloses volumes of positive potential ≥30 kT/e, as in panel A. Note that Asn300 in Figure 2 has been removed from both panels A and B for visual clarity.

these calculations are shown in Figure 9. At the top (Figure 9A) is a diagram of the active site of WT enzyme showing the region most positively charged. It shows that there is a volume of positive field over the pyrimidine portion of the isoalloxazine ring, with a separate volume around Arg220 and Arg214 (holding the carboxyl of the substrate). In Figure 9B is a similar diagram for the mutant enzyme. The field about the active site of the mutant enzyme has strongly positive areas around N1 and C2 of the flavin and around Arg220 and Arg214, just as in WT-PHBH, but is even more extensive in the area over the N10/N1/C2−O of the isoalloxazine ring. This observation is not surprising when the mutation removes a negative charge from behind the pyrimidine ring. Our calculations did not reveal the small area of net positive potential around a segment of the proton network in WT-PHBH that had been calculated in the study of Lys297Met-PHBH (*6*) using an earlier program [DelPhi (*24*)] for solving the Poisson−Boltzmann equations. Rather, our current analysis shows a slightly negative potential around the H-bonds between Tyr201 and Tyr385 in WT-PHBH that is not changed by the mutation. It is clear that an increased electrostatic field that can enhance the stability of the flavin alkoxide leaving group during hydroxylation does correlate with the increased rate of oxygen transfer, even though the pK_a of the substrate is less favorable for phenolate formation than in WT-PHBH. We cannot say if the rate of hydroxylation is increasing with increasing pH and increased phenolate formation because it is too fast to measure. With PHBH where FAD has been replaced by 8-Cl-FAD, a substantial increase in the rate of oxygen transfer to pOHB was also observed (*25*). This rate enhancement is probably due to the same overall explanation as for Glu49Gln-PHBH—an increased stability of the flavin alkoxide leaving group during the process of oxygen transfer. With 8-Cl-FAD PHBH, the increased stability comes from the electron-withdrawing properties of the chlorine substituent in the isoalloxazine ring (*25*).

It is surprising that the pK_a of pOHB is not lowered in the mutant enzyme as it is in WT-PHBH. It is clear that this mutant enzyme does not display the pK_a of about 6.2 in the rate constant for the reduction half of catalysis as is found with WT-PHBH (*3*) and which is attributed to His72 at the end of the proton network. Rather, there is probably a higher pK_a that may correspond to the pK_a of pOHB bound in the oxidized enzyme—results show that this pK_a is >9.5 (Table 1). This behavior is similar to WT-PHBH with substrate analogues such as 2,4-dihydroxybenzoate (*19*). This change in the pK_a of pOHB in the mutant enzyme is not due to a disruption of the proton network that has been shown to regulate aspects of catalysis in PHBH (*3*) because reduction occurs at high rates at high pH (Figure 4), and the oxygen reaction (at all pH values studied) behaves the same as forms

of PHBH known to have an intact proton network (unpublished results). The factors that control the pK_a of pOHB in the active site of the oxidized enzyme must include not only the electrostatic environment (*6*) and the proton network (*3*) but also the equilibrium between interconverting enzyme conformations. The open and out conformations (see below) both have some solvent contact with the phenol of bound pOHB, but the closed/in conformation does not. Thus, a low pK_a (5.8) is found in a mutant that favors the out conformation (*26*), and conversely, a high pK_a (>9.5) is found in a mutant that favors the closed/in conformation (Ala45Gly—unpublished results).

Our results in this paper strongly reinforce the original hypothesis (*6*) that the electrostatic field supports catalysis by enhancing oxygen transfer as well as by stabilizing the reduced flavin in the in conformation for the oxygen reactions. A relationship between the electrostatic field and the pK_a of pOHB bound in the enzyme involves a more complex interplay of factors than had originally been thought. Over the past few years, there have been very few experimentally documented examples of the role of electrostatic potential in the function of proteins. Charge interactions over considerable distances have been implicated in some very high rates of association between proteins and ligands (*27*). A group of negatively charged residues around FMN in an environment of lowered dielectric constant are largely responsible for the low redox potential of flavodoxins (ref *28* and references therein). By comparison, after extensive analysis, it has been much more difficult to establish the contribution of electrostatics to the function of protein disulfide isomerases (*29*, *30*). Kortemme et al. (*29*) thought they established that electrostatic interactions were essential to the low thiol pK_a essential to protein disulfide isomerase activity. Then, Jacobi et al. (*30*) could find no experimental relationship between the low thiol pK_a in the *E. coli* enzyme and charged residues in the immediate environment. It is easy to speculate about electrostatic functions in proteins from crystal structures, but it is much more difficult to demonstrate the validity of these claims.

The most unexpected property of Glu49Gln-PHBH is the slow binding process in forming a complex with pOHB (Figure 8A,B) and a corresponding slow release of pOHB, which is shown by the partial retention of pOHB on the mutant enzyme after passage through a gel filtration column and a slow phase of 0.3 s^{-1} (independent of 2,4-DOHB concentration) due to dissociation of pOHB when displaced by 2,4-DOHB from the complex with oxidized mutant enzyme. Slow binding of pOHB is the primary cause of the low turnover numbers for this mutant enzyme (Table 1). If the mutant enzyme did not have this property, it would behave much like WT-PHBH in turnover, except at pH values less than 8.0, where the rate of reduction is significantly slower than that with WT-PHBH. Once the substrate is bound to Glu49Gln-PHBH, the rest of catalysis proceeds in a manner very similar to WT. Thus, the conformational switch between the in and the out forms (*3*) performs normally, except for a different dependence on pH (as discussed previously). The functional significance of the protein conformational switch that moves the flavin within the protein structure has been studied in detail (refs *17* and *31* and references therein). The reductive and oxidative half-reactions (Figure 1) are combined to provide efficient catalysis through the coordinated and rapid movement of the isoalloxazine by the protein. When flavin movement in the active site is prevented by covalent attachment of the isoalloxazine to the protein (*17*, *32*), catalysis by the enzyme is nearly absent. The evidence for a relationship between the movement of the flavin and the binding of substrate and release of product has been less convincing.

Recently, strong kinetic evidence has been collected for at least three conformational states of PHBH in the catalytic process (*33*). These observations were possible through studying WT-PHBH with the natural FAD replaced by 8-SH-FAD. In this form of the enzyme (still a functioning hydroxylase), there is a combination of relatively slow interconversions of conformations associated with readily measured spectral changes. In the paper by Ortiz-Maldonado et al. (*33*), the conformational states were interpreted in terms of three different positions of the isoalloxazine in the protein. However, since that publication, a new open conformation of PHBH has been established from the structure of Arg220Gln-PHBH [ref *4* and introductory paragraphs]. This open conformation provides a convincing state of PHBH for pOHB to obtain access to its buried binding site. It is a testament to the crystallographers that an open conformation (involving relative domain movements) was predicted as necessary for substrate binding when the first complete crystal structure of PHBH was published in 1983 (*15*). In the open conformation, the flavin is in an environment different from either the in or the out forms (*4*). Indeed, it is likely that PHBH from some organisms prefers to adopt the open conformation in the absence of ligands such as pOHB. It has been noted that isolates from some *Rhodococccus* species have a marked blue-shifted visible flavin absorbance spectrum (*34*), a feature also seen with Arg220Gln-PHBH (*4*). Thus, the three conformations observed in the 8-SH-FAD form of PHBH can now be interpreted as the open, closed (or in), and out forms of the enzyme. Arg220Gln-PHBH is stabilized in the open form, and it is a particularly poor catalyst (*4*) largely because it reduces very slowly. The implication is that substrate cannot trigger flavin movement and thus reduction until the active site is completely closed.

We propose that Glu49Gln-PHBH is kinetically stabilized in both the open and the closed conformations, in roughly equal amounts, so that they interconvert only slowly. This is analogous to the properties of WT-PHBH with 8-SH-FAD (*33*) as discussed previously. As a consequence, the free enzyme, when reduced, should form some transiently stabilized flavin hydroperoxide when it reacts with oxygen because some of the enzyme is kinetically trapped in the closed/in conformation. This is exactly what is observed with this mutant enzyme (Figure 10). The initial reaction with oxygen results in a mixture of oxidized enzyme and flavin-C4a-hydroperoxide that subsequently decomposes at a rate of 1.3 s^{-1}. By comparison, reduced WT-PHBH without substrate only forms oxidized enzyme (*21*), presumably because it can rapidly interconvert between open and closed conformations. The WT enzyme can be forced into stabilizing some flavin-C4a-hydroperoxide (and thus kinetically stabilizing the in/closed conformation) by binding anions in the active site (*17*, *21*). We have also found that reduction of free Glu49Gln-PHBH by NADPH (unlike with pOHB bound) occurs in two distinct phases widely separated in rates, and this is consistent with two forms of the enzyme.

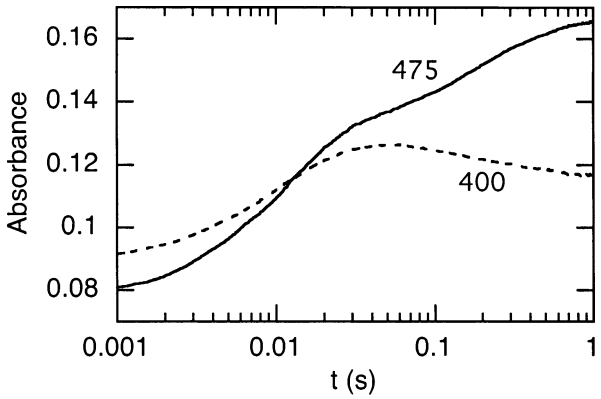

FIGURE 10: Absorbance traces that illustrate the reaction between reduced Glu49Gln-PHBH and oxygen without pOHB. A solution of 19 μM reduced enzyme in 50 mM MOPS buffer, pH 6.5 and 4 °C was mixed with solutions of the same buffer containing different concentrations of oxygen. Two phases are observed in the reaction (with 0.63 mM oxygen) as shown by the traces at different wavelengths as marked. The faster phase has a linear dependence upon oxygen concentration (not shown). From a plot of the observed rates of the first phase against oxygen concentration, a second-order rate constant of 4.3×10^4 M^{-1} s^{-1} was calculated (4-fold slower than that of the mutant enzyme when pOHB is bound in the active site). The slower phase had a rate constant of 1.3 s^{-1} and was independent of oxygen concentration. Analysis of the traces showed that about 40% of the enzyme formed a transiently stable flavin-C4a-hydroperoxide in the reaction (characterized by the peak in absorbance at 400 nm during the reaction).

When pOHB binds to the mutant enzyme, at least two different phases are observed (Figure 8A). The faster, concentration-dependent phase can now be interpreted as binding to the open conformation and the slower phase to the interconversion between the closed form and the open form (that part of the enzyme population that was initially closed) that is required to complete the binding of pOHB. We were not able to resolve the slow phase into more than one process because of the instability of the mutant and the small signal measured in both absorbance and fluorescence. However, more than one phase would be expected on the basis of the model of WT-PHBH with 8-SH−FAD. For example, it should be possible to observe the rate of the conformational change from open to closed/in. Once pOHB is bound in the closed conformation, the mutant enzyme can act as an excellent catalyst. The rate-determining step in turnover of Glu49Gln-PHBH seems to be controlled by the rates that the mutant changes conformations between closed and open. Indeed, we found good agreement between the turnover rate (Table 1) and the rate of the slow step in binding pOHB when that slow step was much slower than any other step in the catalytic cycle (pH 6.5).

ACKNOWLEDGMENT

The authors wish to dedicate this paper to the late Prof. Vincent Massey who spent a substantial fraction of his time for 35 years trying to understand the extraordinary complexity of oxygen reactions in biology.

REFERENCES

1. Entsch, B., and vanBerkel, W. J. H. (1995) *FASEB J. 9*, 476−483.
2. Palfey, B. A., and Massey,V. (1998) in *Comprehensive Biological Catalysis, Volume III* (Sinnott, M., Ed.) pp 83−154, Academic Press, San Diego.
3. Palfey, B. A., Moran, G. R., Entsch, B., Ballou, D. P., and Massey, V. (1999) *Biochemistry 38*, 1153−1158.
4. Wang, J., Ortiz-Maldonado, M., Entsch, B., Massey, V., Ballou, D. P., and Gatti, D. L. (2002) *Proc. Natl. Acad. Sci. U.S.A. 99*, 608−613.
5. Nakamura, H. (1996) *Q. Rev. Biophys. 29*, 1−90.
6. Moran, G. R., Entsch, B., Palfey, B. A., and Ballou, D. P. (1997) *Biochemistry 36*, 7548−7556.
7. Palfey, B. A., Entsch, B., Ballou, D. P., and Massey, V. (1994) *Biochemistry 33*, 1545−1554.
8. Dumas, S. M., Cole, L. J., Ortiz-Maldonado, M., Entsch, B., and Ballou, D. P. (2002) in *Flavins and Flavoproteins 2002* (Chapman, S., Perham, R., and Scrutton, N., Eds.) pp 143−148, Rudolf Weber, Berlin.
9. Entsch, B., Palfey, B. A., Ballou, D. P., and Massey, V. (1991) *J. Biol. Chem. 266*, 17341−17349.
10. Moran, G. R., and Entsch, B. (1995) *Protein Exp. Purif. 6*, 164−168.
11. Entsch, B. (1990) *Methods Enzymol. 188*, 138−147.
12. Press, W. H., Teukolsky, S. A., Vettering, W. T., and Flannery, B. P. (1992) in *Numerical Recipes in C, The Art of Scientific Computing*, 2nd ed., pp 683−688, Cambridge University Press, New York.
13. Baker, N. A., Sept, D., Joseph, S., Holst, M. J., and McCammon, J. A. (2001) *Proc. Natl. Acad. Sci. U.S.A. 98*, 10037−10041.
14. Cornell, W. D., Cieplak, P., Bayly, C. I., Gould, I. R., Merz, K. M., Jr., Ferguson, D. M., Spellmeyer, D. C., Fox, T., Caldwell, J. W., and Kollman, P. A. (1995) *J. Am. Chem. Soc. 117*, 5179−5197.
15. Weijer, W. J., Hofsteenge, J., Beintema, J. J., Wierenga, R. K., and Drenth, J. (1983) *Eur. J. Biochem. 133*, 109−118.
16. Shoun, H., Arima, K., and Beppu, T. (1983) *J. Biochem. (Tokyo) 93*, 169−176.
17. Gatti, D. L., Palfey, B. A., Lah, M. S., Entsch, B., Massey, V., Ballou, D. P., and Ludwig, M. L. (1994) *Science 266*, 110−114.
18. Howell, L. G, Spector, T., and Massey, V. (1972) *J. Biol. Chem. 247*, 4340−4350.
19. Ortiz-Maldonado, M., Entsch, B., and Ballou, D. P. (2003) *Biochemistry 42*, 11234−11242.
20. Husain, M., and Massey, V. (1979) *J. Biol. Chem. 254*, 6657−6666.
21. Entsch, B., Ballou, D. P., and Massey, V. (1976) *J. Biol. Chem. 251*, 2550−2563.
22. Husain, M., Entsch, B., Ballou, D. P., Massey, V., and Chapman, P. J. (1980) *J. Biol. Chem. 255*, 4189−4197.
23. Wessiak, A., Schopfer, L. M., and Massey, V. (1984) *J. Biol. Chem. 259*, 12547−12556.
24. Gilson, M., Sharp, K. A., and Honig, B. (1988) *J. Comput. Chem. 9*, 327−335.
25. Ortiz-Maldonado, M., Ballou, D. P., and Massey, V. (1999) *Biochemistry 38*, 8124−8137.
26. Moran, G. R., Entsch, B., Palfey, B. A., and Ballou, D. P. (1996) *Biochemistry 35*, 9278−9285.
27. Stroppolo, M. E., Falconi, M., Caccuri, A. M., and Desideri, A. (2001) *Cell. Mol. Life Sci. 58*, 1451−1460.
28. Hoover, D. M., Drennan, C. L., Metzger, A. L., Osborne, C., Weber, C. H., Pattridge, K. A., and Ludwig, M. L. (1999) *J. Mol. Biol. 294*, 725−743.
29. Kortemme, T., Darby, N. J., and Creighton, T. E. (1996) *Biochemistry 35*, 14503−14511.
30. Jacobi, A., Huber-Wunderlich, M., Hennecke, J., and Glockschuber, R. (1997) *J. Biol. Chem. 272*, 21692−21699.
31. Palfey, B. A., Basu, R., Frederick, K. K., Entsch, B., and Ballou, D. P. (2002) *Biochemistry 41*, 8438−8446.
32. Palfey, B. A., Ballou, D. P., and Massey, V. (1997) *Biochemistry 36*, 15713−15723.
33. Ortiz-Maldonado, M., Ballou, D. P., and Massey, V. (2001) *Biochemistry 40*, 1091−1101.
34. Jadan, A. P., van Berkel, W. J. H., Golovleva, L. A., and Golovlev, E. L. (2001) *Biochemistry (Moscow) 66*, 898−903.
35. Gibson, Q. H., Swoboda, B. E. P., and Massey, V. (1964) *J. Biol. Chem. 239*, 3927−3934.

BI030193D